

Eshelby-Mori-Tanaka and the Extended Mixture Rule Approaches for Nonlocal Vibration of Piezoelectric Nanocomposite Plate with Considering Surface Stress and Magnetic Field Effects

M. Mohammadimehr^{a*}, B. Rosta Navi^a, A.Ghorbanpour Arani^{a,b}

^aDepartment of Solid Mechanics, Faculty of Mechanical Engineering, University of Kashan, Kashan, Iran

^bInstitute of Nanoscience & Nanotechnology, University of Kashan, Kashan, Iran

Article history:

Received 7/7/2014

Accepted 2/8/2014

Published online 1/9/2014

Keywords:

Vibration analysis

Piezoelectric nanocomposite plate

Surface stress effect

Agglomeration effect

*Corresponding author:

E-mail address:

mmohammadimehr@

kashanu.ac.ir

Phone: +983155912423

Fax: +983155912424

Abstract

In this research, the surface stress effect on the nonlocal vibration of piezoelectric square plate reinforced by single walled carbon nanotubes (SWCNTs) based on classical plate theory (CPT) and first order shear deformation theory (FSDT) is presented. The elastic properties of piezoelectric nanocomposite plate are estimated by Eshelby-Mori-Tanaka and the extended mixture rule approaches. The motion equations of nanocomposite plate are obtained using Hamilton's principle. The Navier's type solution is used to solve these equations. There is the best agreement between the obtained analytical results and other literature results. Then the effects of various parameters such as elastic foundation, surface stress, agglomeration, applied voltage and magnetic field on the nonlocal natural frequency of piezoelectric square nanocomposite plate are investigated. It is concluded that the non-dimensional frequency ratio decreases with increasing the SWCNT volume fraction in the inclusion (agglomeration effect), nonlocal parameter and residual surface stress constant for both CPT and FSDT. Also it is seen that a change in the applied voltage, magnetic field intensity, elastic foundation parameters and surface density leads to increase the non-dimensional frequency ratio.

2014 JNS All rights reserved

1. Introduction

The mechanical behavior of materials at the atomic and molecular scales is investigated in nano science framework. As dimensions of material become smaller, the material properties such as

strength, high electrical conductivity, density, etc. change dramatically. Nowadays, with the development of technology and probable applications of nano materials with unique

properties, nano-materials have been taken into consideration and these materials have been used numerous application such as nano-ceramic superconductors, nano-electro-mechanical systems, nano-medicine, nano textile, and etc. In this regard, carbon nanotubes (CNTs) as single and multi-layers were found in many applications due to their high tensile strength (100 times the strength of steel), high thermal conductivity and excellent electrical conductivity. The unique properties of CNTs have made it possible to be used in many aspects including fuel cells, reinforcement of composites, electromechanical devices, nanomachines and etc [1]. Also because of the excellent thermal and electrical conductivity of CNTs in comparison with other materials, they can be used as filler in polymer composites and extremely improve their properties.

In recent decades, many researchers have investigated the vibrational behavior of nano-plate. Murmu and Pradhan [2] studied the nonlocal plate model for free in-plane vibration of nano-plates using separation of variables. They concluded that without considering the small length scale effect, the classical (local) plate has over estimated results for the free in-plane vibration, also the nonlocal effect on it for the square-type nano-plates is higher than that of on the strip- type nano-plates (nanoribbons). Aghababaei and Reddy [3] presented the analytical solutions of bending and free vibration of a simply supported rectangular plate via nonlocal third-order shear deformation plate theory (TSDPT). They found that increasing of the nonlocal parameter decreases the natural frequencies and increases the deflection of plate. Also difference between results of nonlocal theory and local theory is considerable. Ansari et al. [4] studied the nonlocal vibrations of multi-layered graphene sheets (MLGS) surrounding by elastic

medium using finite element model. They concluded that difference between the natural frequencies in high aspect ratios can be neglected. Also they found that the natural frequencies increase with an increase in the value of elastic medium and the natural frequencies are more affected by the small length scale particularly in higher vibration modes. Ghorbanpour Arani et al. [5] obtained the natural frequencies of the double walled carbon nanotubes (DWCNT) embedded in an elastic medium using the Rayleigh–Ritz method. They showed that the elastic medium increases the stability of DWCNT. Wang et al. [6] investigated the vibration behavior of the double-layered nano-plates considering thermal effect via the nonlocal continuum theory. They concluded that as the half wave number increases, the effect of small scale and thermal effect on the natural frequencies are more considerable. Ansari and Sahmani [7] presented the free vibration behavior of nano-plates considering the surface stress effects based on CPT and FSDT. They showed that the surface stress effect parameter has more considerable effect on the natural frequency of nano-plate for both theories. Also fundamental frequency of the nano-plate decreases with non-positive value of the surface Lamé constants and vice versa for positive of the surface Lamé constants. Furthermore, fundamental frequency decreases with an increase of the residual surface stress. Wang et al. [8] studied the surface energy effects on the nonlocal vibration of Kirchhoff and Mindlin nanoscale plates for simply supported boundary conditions. They showed that the surface energy effect on the natural frequencies of the nano-plates is more considerable and the natural frequency of the nano-plates increases considering the surface energy particularly for lower frequencies but the nonlocal parameter has

reduction effect on the natural frequency and this reduction is higher for higher vibration mode numbers. Jomehzadeh and Saidi [9] used decoupling the displacement field equations theory for three dimensional vibration analysis of nano-plate via nonlocal elasticity theory. They employed Navier's type solution and Fourier series technique for extending analytical three dimensional solution of a nano-plate. They concluded that the non-dimensional frequency decreases with increasing of the thickness to length ratio in constant nonlocal parameter and this decrease in the second mode is higher than that of in the first mode. Navier and Levy solution methods for buckling and vibration of nano-plates using nonlocal elasticity theory for CPT are carried out by Aksencer and Aydogdu [10]. Electro-thermo-nonlocal axial vibration analysis of single-walled boron nitride nanorods (SWBNRs) is studied by Mohammadimehr and Rahmati [11]. They concluded that effect of the small scale on the natural frequencies is higher in lower aspect ratios and higher natural frequencies. Aksencer and Aydogdu [12] studied Navier's solution for the nonlocal forced vibration of single layered graphene sheets (SLGS). They showed that the nonlocal dynamic deflection is higher than the local dynamic deflection and the dynamic deflection decreases with increasing of aspect ratio of SLGS and the nonlocal parameter. An analytical solution obtained for vibration of SLGS resting on Pasternak foundation with modified couple stress theory by Akgz and Civalek [13]. They found that the normalized natural frequencies decreases with increasing the aspect ratio of SLGS and vice versa for increasing of the length to thickness ratio and material length scale parameter effect on the natural frequencies decreases as values of Winkler and shear modulus parameters increases. Vibration behavior of rectangular SLGS as a nanomechanical

sensor based on CPT using Galerkin method is investigated by Shen et al. [14]. They concluded that the natural frequencies of SLGS decrease with an increase in the mass of nanoparticle or with closing it to center of SLGS. By existence of the nonlocal parameter, the natural frequency of SLGS decreases. The natural frequency of SLGS has more changes for the lower side lengths of the SLGS with presence of nanoparticle. Shakouri et al. [15] investigated the small scale effect on the flexural vibration of SLGS based on atomistic structural mode and couple stress theory. They used the general weak form Galerkin method for free vibration analysis with in-plane pre-stress loads and environmental stiffness. Their studies showed that for atomistic structural model, the frequencies of graphene sheets more affected by in-plane pre-stress loads and environmental stiffness. Hashemi et al. [16] extended analytical nonlocal free vibration of Mindlin rectangular nano-plates for Levy-type boundary conditions. They employed the potential functions and separation of variable method for the displacement variables decoupling. They showed that the difference between nonlocal and local frequencies of nano-plate is important in the high nonlocal parameter value and the frequency ratio decreases with an increase in the nonlocal parameter and mode number. Wang [17] studied the bending and vibration of nano-plates considering the surface effect by finite element method based on Kirchhoff and Mindlin plate theories. They found that surface stress effect play an important role on the fundamental frequency particularly in smaller thickness for both Kirchhoff and Mindlin plate theories. Rahmati and Mohammadimehr [18] investigated the vibration analysis of non-uniform and non-homogeneous boron nitride nanorod embedded in an elastic medium under combined

loadings using differential quadrature method (DQM). They indicated that the non-dimensional frequency ratio of non-homogeneous boron nitride nanorod decreases with presence of electro-thermal loadings and effect of them on the non-dimensional frequency ratio is higher in short nanorods and higher nonlocal parameter. Malekzadeh and Shojaee [19] developed two-variable refined plate theory for nonlocal free vibration of nano-plates with different types of boundary conditions using the differential quadrature method (DQM). They also obtained analytical solution for simply supported boundary conditions. They concluded that this theory can be compared with FSDT and higher order shear deformable theory (HSDT). Increasing the nonlocal parameter and the aspect ratio of the nano-plates has decreasing effect on the natural frequency parameter. The nonlocal transverse vibration of SLGS embedded in elastic foundation under in-plane magnetic field is investigated by Murmu et al. [20] for simply supported boundary conditions. They found that the frequency parameter of square SLGS increases with in-plane magnetic field parameter and also the frequency in higher modes is more affected by the nonlocal parameter than in-plane magnetic field parameter. Thermo-electro-mechanical vibration of simply supported piezoelectric rectangular nano-plates via the nonlocal theory and CPT are considered by Liu et al. [21]. They concluded that the influence of thermal- electro-mechanical loadings on the natural frequencies of piezoelectric nano-plates is very significant. Moreover the nonlocal parameter effect has reduction effect on the natural frequencies. Zhang et al. [22] studied the surface effect on nano-piezoelectric plates. They used material properties proposed by Millere and Shenoy. They concluded that with the surface stress effect the resonant natural frequency of

nano-piezoelectric plates is higher than that of without considering the surface stress effect.

Pradhan and Kumar [23] illustrated the vibration behavior of orthotropic graphene sheets with various boundary conditions using DQM via nonlocal elasticity theory. Their results indicated that the non-dimensional frequency of isotropic plate is greater than that of the orthotropic plate. Malekzadeh et al. [24] investigated the free vibration of orthotropic arbitrary straight-sided quadrilateral nano-plates based on FSDT using the DQM. They showed that for the same thickness, the small scale effect on the frequency parameter of the quadrilateral nano-plates increases more than those of the rectangular one. Ghorbanpour Arani et al. [25] presented the buckling analysis of laminated composite rectangular plates reinforced by SWCNTs using analytical and finite element methods. Mori-Tanaka approach is employed to obtain the elastic properties of laminated composite rectangular plates. The critical buckling load decreases with increasing of CNT orientation angle .

Pouresmaeeli et al. [26] presented Navier's type solution for free vibration of the double-orthotropic nano-plates surrounded by elastic foundation for in-phase, out of phase and stationary modes. Their results indicated that the non-dimensional frequency of orthotropic plate is smaller than that of isotropic plate. Also they showed that the non-dimensional frequency of double-orthotropic nano-plates increases with increasing of elastic foundation and this increase for out of phase vibration mode is higher than other vibration modes. Nonlocal vibration analysis of orthotropic nano-plates with thickness variation for different boundary conditions is studied by Shahidi et al. [27]. They computed the size dependent natural frequencies of non-uniform nano-plates based on

CPT with finite element method. They showed that the natural frequencies increases with increasing of thickness and this increase are greater in higher mode number .

Vibrations of carbon nanotube-reinforced composites (CNTRC) with Eshelby–Mori–Tanaka approach and equivalent continuum model is studied by Formica et al. [28]. The matrix material of composite is assumed rubber, concrete and epoxy. They showed that the frequencies of CNTRC increase with increasing of CNT orientation angle and the volume fraction of CNT. Khan et al. [29] investigated the vibration damping behavior of epoxy nanocomposites and carbon fiber reinforced polymer composites (CFRPs) including multi-walled carbon nanotubes (MWCNTs) by the free and forced vibration tests. They reported that damping ratio of CFRPs is lower than that of epoxy nanocomposites. Damping ratio of both epoxy nanocomposites and CFRPs are improved by CNTs both in mode vibration of 1st and 2st and this improvement is higher for epoxy nanocomposites than CFRPs, also damping ratio of CFRPs increases with increasing of CNTs. Lei et al. [30] investigated the free vibration analysis of functionally graded nanocomposite plates reinforced by SWCNTs using the element-free kp-Ritz method in thermal environment based on FSDT with different boundary conditions. The material properties of the functionally graded nanocomposite plates are varied through the thickness direction by linear function of the volume fraction of CNTs. They used Eshelby–Mori–Tanaka and extended mixture rule approaches for material property estimation of CNTRC plate. They showed that the non-dimensional fundamental frequency of various types of CNTRC plates increases with an increase

of CNT volume fraction and width to thickness ratio.

In this article the free vibration behavior of piezoelectric square nanocomposite plate reinforced by SWCNTs based on CPT and FSDT is investigated. Influences of nonlocal parameter, surface stress, SWCNT volume fraction, SWCNT orientation angle, aspect ratio, applied voltage, magnetic field and elastic foundation on vibration behavior of piezoelectric plate reinforced by SWCNTs are studied. Material properties of piezoelectric square plate reinforced by SWCNTs are predicted by Eshelby-Mori-Tanaka and the extended mixture rule approaches. Also stress surface and agglomeration effects on the free vibration of piezoelectric nanocomposite plate reinforced by SWCNTs are investigated.

2. Various approaches to obtain the elastic properties of nanocomposite

In this section, Eshelby-Mori-Tanaka (E-M-T) and the extended mixture rule (E-M-R) approaches to obtain material properties of piezoelectric nanocomposite plate reinforced by SWCNTs are presented.

2.1. The extended mixture rule approach

In E-M-R approach, the material properties of nanocomposite are defined as the following equation [31].

$$E_1 = \eta_1 E_f V_f + E_m V_m \quad (1)$$

$$\frac{\eta_2}{E_2} = \frac{V_f}{E_{2f}} + \frac{V_m}{E_m} \quad (2a)$$

$$\frac{\eta_3}{G_2} = \frac{V_f}{G_f} + \frac{V_m}{G_m} \quad (2b)$$

where η_1 , η_2 and η_3 are constants which are defined by the molecular dynamic simulations and usually vary from 0.7 to 1. E_{1f} and E_{2f} are longitudinal and transverse elastic moduli, respectively.

2.2. Eshelby-Mori-Tanaka approach

In this approach, it is assumed that nanocomposite reinforced by straight and long CNT fibers; also the fibers are uniformly distributed in the isotropic matrix of composite. The stiffness coefficients are stated as follows [32].

$$\begin{aligned}
 Q_{11} &= \frac{E_m c_m (1+V_f - V_m \nu_m) + 2V_f V_m (k_f n_f - l_f) (1+\nu_m) (1-2\nu_m)}{(1+\nu_m) \{ 2V_m k_f (1-\nu_m - 2\nu_m^2) + E_m (1+V_f - 2\nu_m) \}} + \\
 &\quad \frac{E_m [2V_m^2 k_f (1-\nu_m) V_f n_f (1+V_f - 2\nu_m) - 4V_m l_f \nu_m]}{2V_m k_f (1-\nu_m - 2\nu_m^2) + E_m (1+V_f - 2\nu_m)} \\
 Q_{22} &= \frac{E_m \{ E_m V_m + 2k_f (1+\nu_m) [V_f (1-2\nu_m) + 1] \}}{2(1+\nu_m) \{ 2V_m k_f (1-\nu_m - 2\nu_m^2) + E_m (1+V_f - 2\nu_m) \}} + \\
 &\quad \frac{E_m [E_m V_m + 2m_f (3+V_f - 4\nu_m) (1+\nu_m)]}{2(1+\nu_m) \{ E_m [V_f + 4V_f (1-\nu_m)] + 2m_f (3+V_f - 4\nu_m^2) \}} \\
 Q_{12} &= \frac{E_m \{ V_m \nu_m [E_m + 2k_f (1+\nu_m)] + 2V_f l_f (1-\nu_m^2) \}}{(1+\nu_m) [2V_m k_f (1-\nu_m - 2\nu_m^2) + E_m (1+V_f - 2\nu_m)]} \\
 Q_{44} &= \frac{E_m [E_m V_m + 2m_f (3+V_f - 4\nu_m) (1+\nu_m)]}{2(1+\nu_m) \{ E_m [V_m + 4V_f (1-\nu_m)] + 2m_f V_m (3+V_f - 4\nu_m^2) \}} \quad (3) \\
 Q_{55} = Q_{66} &= \frac{E_m [E_m V_m + 2p_f (1+V_f) (1+\nu_m)]}{2(1+\nu_m) [E_m (1+V_f) + 2V_m p_f (1+\nu_m)]}
 \end{aligned}$$

where ν_m is the Poisson's ratio of matrix and k_f , n_f , m_f and p_f are the Hill's elastic moduli for the CNTs [32].

3. The agglomeration effect of SWCNT

The SWCNT fibers are accumulated in polymeric matrix due to lower flexural strength of CNT in its

radial direction. Because of it, accumulation of CNT in several zone of nanocomposite matrix is higher than in other zones. For specification of this phenomenon, the spherical region of accumulation is called inclusion and two material constants K and G both inside and outside of inclusion are defined as the following equations [32]:

$$\begin{aligned}
 K_{in} &= K_m + \frac{(\delta_f - 3k_m \alpha_f) V_f \zeta}{3(\xi - V_f \zeta + V_f \zeta \alpha_f)} \\
 K_{out} &= K_m + \frac{V_f (\delta_f - 3k_m \alpha_f) (1-\zeta)}{3[1-\xi - V_f (1-\zeta) + V_f (1-\zeta) \alpha_f]} \\
 G_{in} &= G_m + \frac{V_f \zeta (\eta_f - 2G_m \beta_f)}{2(\xi - V_f \zeta + V_f \zeta \beta_f)} \\
 G_{out} &= G_m + \frac{V_f (\eta_f - 2G_m \beta_f) (1-\zeta)}{2[1-\xi - V_f (1-\zeta) + V_f (1-\zeta) \theta_f]} \quad (4)
 \end{aligned}$$

where ξ and ζ are inclusion volume to total volume ratio and SWCNT volume fraction in the inclusion ratios, respectively. If SWCNT fibers are uniformly distributed in matrix then ξ is equal to 1 and if thorough fiber agglomeration is happened then ξ is equal to 1. In Eq. (4), δ_f , α_f , β_f and η_f are written as follows [32]:

$$\begin{aligned}
 \alpha_f &= \frac{3(k_m + G_m) + k_f + l_f}{3(k_m + G_m)} \\
 \beta_f &= \frac{1}{5} \left\{ \frac{4G_m + 2k_f + l_f}{3(k_f + G_m)} + \frac{4G_m}{G_m + p_f} + \frac{2[G_m(3k_m + G_m) + G_m(3k_m + 7G_m)]}{G_m(3k_m + G_m) + m_f(3k_m + 7G_m)} \right\} \\
 \delta_f &= \frac{1}{2} \left\{ n_f + 2l_f + \frac{(2k_f + l_f)(3k_m + 2G_m - l_f)}{G_m + k_f} \right\} \\
 \eta_f &= \frac{1}{5} \left\{ \frac{\frac{2}{3}(n_f - l_f) + \frac{8G_m p}{G_m + p_f} + 8m_f G_m (3k_m + 4G_m)}{3k_m(m_f + G_m) + G_m(7m_f + G_m)} + \frac{2(k_f - l_f)(l_f + 2G_m)}{3(k_f + G_m)} \right\} \\
 \nu_{out} &= \frac{(3k_{out} - 2G_{out})}{2(3k_{out} + G_{out})} \\
 \alpha &= \frac{1 + \nu_{out}}{3(1 - \nu_{out})} \\
 \beta &= \frac{2(4 - 5\nu_{out})}{15(1 - \nu_{out})} \\
 k &= k_{out} \left[1 + \frac{\xi \left(\frac{k_{in}}{k_{out}} - 1 \right)}{1 + \alpha(1 - \xi) \left(\frac{k_{in}}{k_{out}} - 1 \right)} \right] \\
 G &= G_{out} \left[1 + \frac{\xi \left(\frac{G_{in}}{G_{out}} - 1 \right)}{1 + \beta(1 - \xi) \left(\frac{G_{in}}{G_{out}} - 1 \right)} \right] \\
 E &= \frac{9kG}{3k + G} \quad \nu = \frac{3k - G}{6k + 2G}
 \end{aligned} \tag{5}$$

4. The motion equations of nanocomposite plate based CPT and FSDT

If the mid-plane displacements of the plate in the x and y directions are zero, The displacement fields of CPT and FSDT can be stated as follows:

$$\begin{aligned}
 u(x, y, z) &= z\varphi_x \\
 v(x, y, z) &= z\varphi_y \\
 w(x, y, z) &= w(x, y)
 \end{aligned} \tag{6}$$

where u, v, and w are the components of displacement fields along x, y and z coordinates, respectively. φ_x and φ_y are rotation components about to x, y coordinates. It can be noticed that φ_x and φ_y are equal to $-\partial w(x, y) / \partial x$ and $-\partial w(x, y) / \partial y$ for CPT, respectively.

The kinematic equations are written as:

$$\begin{aligned}
 \epsilon_x &= z \frac{\partial \phi_x}{\partial x}, \quad \epsilon_y = z \frac{\partial \phi_y}{\partial y} \\
 \epsilon_z &= 0, \quad \gamma_{yz} = \phi_y + \frac{\partial w}{\partial y}, \quad \gamma_{xz} = \phi_x + \frac{\partial w}{\partial x} \\
 \gamma_{xy} &= z \left(\frac{\partial \phi_x}{\partial y} + \frac{\partial \phi_y}{\partial x} \right)
 \end{aligned} \tag{7}$$

The constitutive equations for the piezoelectric plate can be written as:

$$\begin{aligned}
 \begin{Bmatrix} \sigma_x \\ \sigma_y \\ \sigma_{yz} \\ \sigma_{xz} \\ \sigma_{xy} \end{Bmatrix} &= \begin{bmatrix} Q_{11} & Q_{12} & 0 & 0 & 0 \\ Q_{12} & Q_{22} & 0 & 0 & 0 \\ 0 & 0 & Q_{44} & 0 & 0 \\ 0 & 0 & 0 & Q_{55} & 0 \\ 0 & 0 & 0 & 0 & Q_{66} \end{bmatrix} \begin{Bmatrix} \varepsilon_x \\ \varepsilon_y \\ \gamma_{yz} \\ \gamma_{xz} \\ \gamma_{xy} \end{Bmatrix} - \\
 &\begin{bmatrix} 0 & 0 & e_{31} \\ 0 & 0 & e_{32} \\ 0 & e_{24} & 0 \\ e_{15} & 0 & 0 \\ 0 & 0 & 0 \end{bmatrix} \begin{Bmatrix} E_x \\ E_y \\ E_z \end{Bmatrix} \quad (8) \\
 \begin{Bmatrix} D_x \\ D_y \\ D_z \end{Bmatrix} &= \begin{bmatrix} 0 & 0 & 0 & e_{15} & 0 \\ 0 & 0 & e_{24} & 0 & 0 \\ e_{31} & e_{32} & 0 & 0 & 0 \end{bmatrix} \begin{Bmatrix} \varepsilon_x \\ \varepsilon_y \\ \gamma_{yz} \\ \gamma_{xz} \\ \gamma_{xy} \end{Bmatrix} + \\
 &\begin{bmatrix} \zeta_{11} & 0 & 0 \\ 0 & \zeta_{22} & 0 \\ 0 & 0 & \zeta_{33} \end{bmatrix} \begin{Bmatrix} E_x \\ E_y \\ E_z \end{Bmatrix} \quad i, j = x, y
 \end{aligned}$$

In the above expressions $\sigma_{ij}, D_i, \varepsilon_{ij}$ and E_i are the stress, electrical displacement, strain and electric field components, respectively. Q_{ij}, e_{ij} and ζ_{ij} are also stiffness matrix, piezoelectric and dielectric coefficients, respectively. The electric field in terms of the electric potential ϕ can be expressed as follows:

$$E_i = -\phi_{,i} \quad (9)$$

The potential function is applied in the thickness direction of the nanocomposite plate. This function must also satisfy Maxwell's equations. This function is considered as follows [33]:

$$\begin{aligned}
 \phi(x, y, z, t) &= -\cos(\pi z / h)\phi(x, y, t) + \\
 &2zV_0 e^{i\omega t} / h \quad (10)
 \end{aligned}$$

In the above equation, V_0 is external applied electrical voltage, $\phi(x, y, t)$ denotes arbitrary function of time and location that will satisfy the Maxwell's equation. ω is the natural frequencies of the nanocomposite plate that becomes zero in buckling mode.

If the carbon nano-fibers in the matrix of the nanocomposite plate have angle α , the coefficients of fundamental relations must be changed as follows:

$$Q' = RQR^{-1}, e' = ReR^{-1}, \zeta' = R\zeta R^{-1} \quad (11)$$

where R is the rotation matrix that is considered as the following form:

$$R = \begin{bmatrix} n^2 & m^2 & 0 & 0 & -2nm \\ n^2 & m^2 & 0 & 0 & 2nm \\ 0 & 0 & n & m & 0 \\ 0 & 0 & -m & n & 0 \\ nm & nm & 0 & 0 & n^2 - m^2 \end{bmatrix} \quad (12)$$

where:

$$\begin{aligned}
 n &= \cos(\alpha) \\
 m &= \sin(\alpha) \quad (13)
 \end{aligned}$$

Energy method and Hamilton's principle are applied to obtain the motion equations of piezoelectric nanocomposite plate reinforced by

SWCNT. Considering the stress surface effect, Hamilton's principle can be stated as follows:

$$\int (\delta T + \delta T^s - \delta W_{ext} - \delta U - \delta U^s) dt = 0 \tag{14}$$

where U , U^s , δT , δT^s and W_{ext} are strain energy, the surface strain energy, kinetic energy, the surface kinetic energy and the work done by the external forces, respectively. Subscript "s" illustrates the surface stress effect.

Variation of strain energy is considered as follows:

$$\delta U = \int_V \left(\sigma_x \delta \epsilon_x + \sigma_y \delta \epsilon_y + \sigma_{xy} \delta \epsilon_{xy} - D_x \delta E_x - D_y \delta E_y - D_z \delta E_z \right) dV \tag{15}$$

Substituting Eqs. (7), (8) and (5) into Eq. (15) and simplifying it, strain energy variation can be written as follows:

$$\delta U = \int_A \left(M_{x,x} \delta \phi_x + 2e_{13} V_0 \frac{\partial^2 w}{\partial x^2} \delta w + M_{y,y} \delta \phi_y + 2e_{23} V_0 \frac{\partial^2 w}{\partial y^2} \delta w + M_{xy,y} \delta \phi_x + M_{xy,x} \delta \phi_y - N_{xz} \delta \phi_x - N_{xz,x} \delta w - N_{yz} \delta \phi_y + N_{yz,y} \delta w \right) dA + \int_A \int_{-h/2}^{h/2} \left(\cos\left(\frac{\pi z}{h}\right) \left(-\frac{\partial D_x}{\partial x}\right) \delta \phi - \cos\left(\frac{\pi z}{h}\right) \frac{\partial D_y}{\partial y} \delta \phi - \frac{\pi}{h} \sin\left(\frac{\pi z}{h}\right) D_z \delta \phi \right) dz dA \tag{16}$$

where N_{ij} and M_{ij} are the resultant forces and moments, respectively, which are defined as:

$$\begin{Bmatrix} N_x \\ N_y \\ N_{xy} \\ N_{xz} \\ N_{yz} \end{Bmatrix} = \int_{-h/2}^{h/2} \begin{Bmatrix} \sigma_x \\ \sigma_y \\ \sigma_{xy} \\ k\sigma_{xz} \\ k\sigma_{yz} \end{Bmatrix} dz, \tag{17}$$

$$\begin{Bmatrix} M_x \\ M_y \\ M_{xy} \end{Bmatrix} = \int_{-h/2}^{h/2} \begin{Bmatrix} \sigma_x \\ \sigma_y \\ \sigma_{xy} \end{Bmatrix} z dz$$

To consider the effect of surface tension is assumed that σ_z varies linearly along the z coordinate. Assuming constant surface properties of the top and bottom layers of the nano-plate, the surface stresses are stated as [7]:

$$\begin{aligned} \sigma_x^s &= \frac{2\nu z}{h(1-\nu)} \left(\tau_s \frac{\partial^2 w}{\partial x^2} + \tau_s \frac{\partial^2 w}{\partial y^2} - \rho_s \frac{\partial^2 w}{\partial t^2} \right) + E_s \epsilon_x + \tau_s \\ \sigma_y^s &= \frac{2\nu z}{h(1-\nu)} \left(\tau_s \frac{\partial^2 w}{\partial x^2} + \tau_s \frac{\partial^2 w}{\partial y^2} - \rho_s \frac{\partial^2 w}{\partial t^2} \right) + E_s \epsilon_y + \tau_s \\ \sigma_{xz}^s &= \tau_s \frac{\partial w}{\partial x} \\ \sigma_{yz}^s &= \tau_s \frac{\partial w}{\partial y} \end{aligned} \tag{18}$$

where E_s , τ_s and ρ_s are the surface Lamé constant, residual stress constant and surface density, respectively. Substituting Eq. (7) into Eq. (18) yields:

$$\begin{aligned} \sigma_x^s &= \frac{2\nu z}{h(1-\nu)} \left(\tau_s \frac{\partial^2 w}{\partial x^2} + \tau_s \frac{\partial^2 w}{\partial y^2} - \rho_s \frac{\partial^2 w}{\partial t^2} \right) + z E_s \frac{\partial \varphi_x}{\partial x} + \tau_s \\ \sigma_y^s &= \frac{2\nu z}{h(1-\nu)} \left(\tau_s \frac{\partial^2 w}{\partial x^2} + \tau_s \frac{\partial^2 w}{\partial y^2} - \rho_s \frac{\partial^2 w}{\partial t^2} \right) + z E_s \frac{\partial \varphi_y}{\partial y} + \tau_s \\ \sigma_{xz}^s &= \tau_s \frac{\partial w}{\partial x} \\ \sigma_{yz}^s &= \tau_s \frac{\partial w}{\partial y} \end{aligned} \tag{19}$$

Variation of the surface strain energy of nanocomposite plate is calculated as follows:

$$\delta U^s = \int_A \left(\sigma_x^s \delta \varepsilon_x + \sigma_y^s \delta \varepsilon_y + \sigma_{xz}^s \delta \varepsilon_{xz} + \sigma_{yz}^s \delta \varepsilon_{yz} \right) dA dz \tag{20}$$

Substituting Eqs. (7) and (19) into Eq. (20) and simplifying it, the following equations can be obtained:

For nano-plate (matrix):

$$\begin{aligned} \delta U^s &= -\frac{\nu \tau_s h^2}{6(1-\nu)} \left(\frac{\partial^3 w}{\partial x^3} + \frac{\partial^3 w}{\partial x \partial y^2} \right) \delta \varphi_x - \frac{\nu \tau_s h^2}{6(1-\nu)} \nabla^4 w \delta w \\ &\quad - \frac{\nu \tau_s h^2}{6(1-\nu)} \left(\frac{\partial^3 w}{\partial y^3} + \frac{\partial^3 w}{\partial y \partial x^2} \right) \delta \varphi_y - 4\tau_s (b+h) \left(\frac{\partial^2 w}{\partial x^2} + \frac{\partial^2 w}{\partial y^2} \right) \delta w \\ &\quad + E_s (bh^2/2 + h^3/6) \left(\frac{\partial^2 \varphi_x}{\partial x^2} \delta \varphi_x + \frac{\partial^2 \varphi_y}{\partial y^2} \delta \varphi_y \right) \\ &\quad + \frac{\nu \rho_s h^2}{6(1-\nu)} \left(\frac{\partial^3 w}{\partial t^2 \partial x} \delta \varphi_x + \frac{\partial^3 w}{\partial t^2 \partial y} \delta \varphi_y \right) \\ &\quad - 2\tau_s (b+h) \left(\frac{\partial w}{\partial x} \delta \varphi_x + \frac{\partial w}{\partial y} \delta \varphi_y \right) \\ &\quad + \frac{\nu \rho_s h^2}{6(1-\nu)} \left(\frac{\partial^4 w}{\partial t^2 \partial x^2} + \frac{\partial^4 w}{\partial t^2 \partial y^2} \right) \delta w \end{aligned} \tag{21}$$

For SWCNT (fibers) [34]:

$$\begin{aligned} \delta U_{cnt}^s &= +4\tau_{scnt} d \left(\frac{\partial^2 w}{\partial x^2} + \frac{\partial^2 w}{\partial y^2} \right) \delta w - \\ &\quad E_{scnt} (3\pi d^3/8) \left(\frac{\partial^2 \varphi_x}{\partial x^2} \delta \varphi_x + \frac{\partial^2 \varphi_y}{\partial y^2} \delta \varphi_y \right) \end{aligned} \tag{22}$$

Kinetic energy variation and surface kinetic energy variation can be expressed as following equations:

$$\begin{aligned} \delta T &= \int_V \rho \left(\frac{\partial u}{\partial t} \frac{\partial \delta u}{\partial t} + \frac{\partial v}{\partial t} \frac{\partial \delta v}{\partial t} + \frac{\partial w}{\partial t} \frac{\partial \delta w}{\partial t} \right) dV \\ &= - \int_V \left(\frac{\rho h^2}{12} \frac{\partial^2 \varphi_x}{\partial t^2} \delta \varphi_x + \rho h \frac{\partial^2 w}{\partial t^2} \delta w + \frac{\rho h^2}{12} \frac{\partial^2 \varphi_y}{\partial t^2} \delta \varphi_y \right) dA \end{aligned} \tag{23}$$

$$\begin{aligned} \delta T^s &= \int_V \rho_s \left(\frac{\partial u}{\partial t} \frac{\partial \delta u}{\partial t} + \frac{\partial v}{\partial t} \frac{\partial \delta v}{\partial t} + \frac{\partial w}{\partial t} \frac{\partial \delta w}{\partial t} \right) dA dz \\ &= - \int_A \rho_s \left((bh^2/2 + h^3/6) \frac{\partial^2 \varphi_x}{\partial t^2} + (bh^2/2 + h^3/6) \frac{\partial^2 \varphi_y}{\partial t^2} + 2(b+h) \frac{\partial^2 w}{\partial t^2} \right) dA \end{aligned} \tag{24}$$

where ρ is density of nanocomposite plate.

Work done by external forces such as Pasternak foundation and the Lorentz force are considered in this research. First Lorentz forces due to the magnetic field that is entered separately in the three coordinate directions are extracted then variation of the work done by these forces is presented.

The electro-dynamic Maxwell's equations for the nanocomposite plate can be written as [35]:

$$\begin{aligned} \vec{h} &= \nabla \times (\vec{U} \times \vec{H}) \\ \vec{J} &= \nabla \times \vec{h} \\ \vec{f}_l &= \eta (\vec{J} \times H) \end{aligned} \tag{25}$$

where U , H and η are the displacement field (u , v , w), the magnetic field and the magnetic permeability, respectively. If the magnetic field (0, 0, Hz), is applied in the thickness of the nanocomposite plate then substituting it in Eq. (25), Lorentz forces are obtained as follows:

$$\begin{aligned} f_{xl} &= \eta H_z^2 \left(\frac{\partial^2 u}{\partial x^2} + \frac{\partial^2 v}{\partial x \partial y} \right) = \eta z H_z^2 \left(\frac{\partial^2 \varphi_x}{\partial x^2} + \frac{\partial^2 \varphi_y}{\partial x \partial y} \right) \\ f_{yl} &= \eta H_z^2 \left(\frac{\partial^2 u}{\partial x \partial y} + \frac{\partial^2 v}{\partial y^2} \right) = \eta z H_z^2 \left(\frac{\partial^2 \varphi_x}{\partial y^2} + \frac{\partial^2 \varphi_y}{\partial x \partial y} \right) \end{aligned} \tag{26}$$

Then variation of the work done by the Lorentz forces is calculated as:

$$\begin{aligned} \delta W_{ext}^{f_l} &= \int_V (f_{xl} \delta u + f_{yl} \delta v) dV \\ &= \int_A \left(\left(\frac{\partial^2 \varphi_x}{\partial x^2} + \frac{\partial^2 \varphi_y}{\partial x \partial y} \right) \delta \varphi_x + \left(\frac{\partial^2 \varphi_x}{\partial y^2} + \frac{\partial^2 \varphi_y}{\partial x \partial y} \right) \delta \varphi_y \right) \frac{\eta h^3}{12} H_z^2 dA \end{aligned} \tag{27}$$

Work done by to the elastic foundation can be written as:

$$\begin{aligned} \delta W_{ext}^{f_p} &= \int_A (f_w \delta w + f_g \delta w) dA \\ &= \int_A (k_w w \delta w - k_g \nabla^2 w \delta w) dA \end{aligned} \tag{28}$$

where k_w and k_g are Winkler spring and Pasternak shear constants, respectively.

Substituting of the obtained relations into Eq. (14) becomes the following equation:

$$\begin{aligned} M_{x,x} + M_{xy,y} - N_{xz} + \frac{\nu h^2 \tau_s}{6(1-\nu)} \left(\frac{\partial^3 w}{\partial x^3} + \frac{\partial^3 w}{\partial x \partial y^2} \right) + \\ \frac{\nu \rho_s h^2}{6(1-\nu)} \frac{\partial^3 w}{\partial t^2 \partial x} - 2\tau_s (b+h) \frac{\partial w}{\partial x} + E_{scut} (3\pi d^3 / 8) \frac{\partial^2 \varphi_x}{\partial x^2} - \\ f_x^l + E_{scut} (3\pi d^3 / 8) \frac{\partial^2 \varphi_x}{\partial x^2} = E_s (bh^2 / 2 + h^3 / 6) \frac{\partial^2 \varphi_x}{\partial x^2} + \\ \left(\frac{\rho h^3}{12} + (bh^2 / 2 + h^3 / 6) \rho_s \right) \frac{\partial^2 \varphi_x}{\partial t^2} \end{aligned} \tag{29a}$$

$$\begin{aligned} M_{y,y} + M_{yx,x} - N_{yz} + \frac{\nu h^2 \tau_s}{6(1-\nu)} \left(\frac{\partial^3 w}{\partial y^3} + \frac{\partial^3 w}{\partial y \partial x^2} \right) + \\ \frac{\nu \rho_s h^2}{6(1-\nu)} \frac{\partial^3 w}{\partial t^2 \partial y} - 2\tau_s (b+h) \frac{\partial w}{\partial y} + E_{scut} (3\pi d^3 / 8) \frac{\partial^2 \varphi_y}{\partial y^2} - \\ f_y^l + E_{scut} (3\pi d^3 / 8) \frac{\partial^2 \varphi_y}{\partial y^2} = E_s (bh^2 / 2 + h^3 / 6) \frac{\partial^2 \varphi_y}{\partial y^2} + \\ \left(\frac{\rho h^3}{12} + (bh^2 / 2 + h^3 / 6) \rho_s \right) \frac{\partial^2 \varphi_y}{\partial t^2} \end{aligned} \tag{29b}$$

$$\begin{aligned} N_{yz,y} + N_{zx,x} + 4\tau_s (b+h) \left(\frac{\partial^2 w}{\partial x^2} + \frac{\partial^2 w}{\partial y^2} \right) + \frac{\nu h^2 \tau_s}{6(1-\nu)} \nabla^4 w \\ + k_w w - k_g \nabla^2 w + f_z^l - 4\tau_{scut} d \left(\frac{\partial^2 w}{\partial x^2} + \frac{\partial^2 w}{\partial y^2} \right) = \\ (\rho h + 2(b+h) \rho_s) \frac{\partial^2 w}{\partial t^2} + \frac{\nu \rho_s h^2}{6(1-\nu)} \left(\frac{\partial^4 w}{\partial t^2 \partial x^2} + \frac{\partial^4 w}{\partial t^2 \partial y^2} \right) \end{aligned} \tag{29c}$$

$$\int_{-h/2}^{h/2} \left(\cos\left(\frac{\pi z}{h}\right) \left(\frac{\partial D_x}{\partial x}\right) \delta\phi + \cos\left(\frac{\pi z}{h}\right) \frac{\partial D_y}{\partial y} \delta\phi + \frac{\pi}{h} \sin\left(\frac{\pi z}{h}\right) D_z \delta\phi \right) dz = C \quad (29d)$$

To consider the small-scale effect, the nonlocal piezoelectricity theory is used. According to this theory, stresses at a small scale can be stated as follows [5]:

$$\begin{aligned} (1 - (e_0 a)^2 \nabla^2) \sigma^{nonlocal} &= \sigma^{local} \\ (1 - (e_0 a)^2 \nabla^2) D^{nonlocal} &= D^{local} \end{aligned} \quad (30)$$

where $e_0 a$ and ∇^2 are the nonlocal parameter and the Laplacian operation, respectively. Using Eq. (30), the nonlocal motion equations are obtained as follows:

$$\begin{aligned} M_{x,x} + M_{y,y} - N_x + \frac{\nu h^2 \tau_s}{6(1-\nu)} \left(\frac{\partial^3 w}{\partial x^3} + \frac{\partial^3 w}{\partial x \partial y^2} \right) + \\ (1 - (e_0 a)^2 \nabla^2) E_s (bh^2 / 2 + h^3 / 6) \frac{\partial^2 \phi_x}{\partial x^2} - \\ 2\tau_s (1 - (e_0 a)^2 \nabla^2) (b+h) \frac{\partial w}{\partial x} + E_{scut} (3\pi d^3 / 8) \frac{\partial^2 \phi_x}{\partial x^2} + \\ (1 - (e_0 a)^2 \nabla^2) f_x^I = \frac{\nu \rho_s h^2}{6(1-\nu)} \frac{\partial^3 w}{\partial t^2 \partial x} + \\ (1 - (e_0 a)^2 \nabla^2) \left(\frac{\rho h^3}{12} + (bh^2 / 2 + h^3 / 6) \rho_s \right) \frac{\partial^2 \phi_x}{\partial t^2} \end{aligned} \quad (31a)$$

$$\begin{aligned} M_{y,y} + M_{x,x} - N_y + \frac{\nu h^2 \tau_s}{6(1-\nu)} \left(\frac{\partial^3 w}{\partial y^3} + \frac{\partial^3 w}{\partial y \partial x^2} \right) + \\ (1 - (e_0 a)^2 \nabla^2) E_s (bh^2 / 2 + h^3 / 6) \frac{\partial^2 \phi_y}{\partial y^2} - \\ 2\tau_s (1 - (e_0 a)^2 \nabla^2) (b+h) \frac{\partial w}{\partial y} + E_{scut} (3\pi d^3 / 8) \frac{\partial^2 \phi_y}{\partial y^2} \end{aligned} \quad (31b)$$

$$\begin{aligned} (1 - (e_0 a)^2 \nabla^2) f_y^I = \frac{\nu \rho_s h^2}{6(1-\nu)} \frac{\partial^3 w}{\partial t^2 \partial y} + \\ (1 - (e_0 a)^2 \nabla^2) \left(\frac{\rho h^3}{12} + (bh^2 / 2 + h^3 / 6) \rho_s \right) \frac{\partial^2 \phi_y}{\partial t^2} \\ N_{y,x} + N_{x,x} + 4\tau_s (1 - (e_0 a)^2 \nabla^2) (b+h) \left(\frac{\partial^2 w}{\partial x^2} + \frac{\partial^2 w}{\partial y^2} \right) + \\ \frac{\nu h^2 \tau_s}{6(1-\nu)} \nabla^4 w + k_w (1 - (e_0 a)^2 \nabla^2) w - k_g (1 - (e_0 a)^2 \nabla^2) \nabla^2 w + \\ (1 - (e_0 a)^2 \nabla^2) f_z^I - 4\tau_{scut} (1 - (e_0 a)^2 \nabla^2) d \left(\frac{\partial^2 w}{\partial x^2} + \frac{\partial^2 w}{\partial y^2} \right) = \end{aligned} \quad (31c)$$

$$\begin{aligned} (1 - (e_0 a)^2 \nabla^2) (\rho h + 2(b+h) \rho_s) \frac{\partial^2 w}{\partial t^2} + \\ \frac{\nu \rho_s h^2}{6(1-\nu)} \left(\frac{\partial^4 w}{\partial t^2 \partial x^2} + \frac{\partial^4 w}{\partial t^2 \partial y^2} \right) \\ (1 - (e_0 a)^2 \nabla^2) \left(\cos\left(\frac{\pi z}{h}\right) \left(-\frac{\partial D_x}{\partial x}\right) \delta\phi - \cos\left(\frac{\pi z}{h}\right) \frac{\partial D_y}{\partial y} \delta\phi - \frac{\pi}{h} \sin\left(\frac{\pi z}{h}\right) D_z \delta\phi \right) = 0 \end{aligned} \quad (31d)$$

Substituting Eqs. (8) and (19) into Eq. (31) yields the following equations:

$$\begin{aligned} \frac{C_{11} h^3}{12} \phi_{x,xx} + \frac{C_{12} h^3}{12} \phi_{y,xy} + bb\phi_{,x} + \frac{C_{66} h^3}{12} \phi_{x,yy} \\ + \frac{C_{66} h^3}{12} \phi_{y,xy} - C_{55} h w_{,x} - C_{55} h \phi_{,x} - cc\phi_{,x} \\ + \frac{\nu h^2 \tau_s}{6(1-\nu)} \left(\frac{\partial^3 w}{\partial x^3} + \frac{\partial^3 w}{\partial x \partial y^2} \right) + E_{scut} (3\pi d^3 / 8) \frac{\partial^2 \phi_x}{\partial x^2} \\ + (1 - (e_0 a)^2 \nabla^2) E_s (bh^2 / 2 + h^3 / 6) \frac{\partial^2 \phi_x}{\partial x^2} \\ - 2\tau_s (1 - (e_0 a)^2 \nabla^2) (b+h) \frac{\partial w}{\partial x} + (1 - (e_0 a)^2 \nabla^2) f_x \\ = (1 - (e_0 a)^2 \nabla^2) \left(\frac{\rho h^3}{12} + (bh^2 / 2 + h^3 / 6) \rho_s \right) \frac{\partial^2 \phi_x}{\partial t^2} \\ + \frac{\nu \rho_s h^2}{6(1-\nu)} \frac{\partial^3 w}{\partial t^2 \partial x} \end{aligned} \quad (32a)$$

$$\begin{aligned} & \frac{C_{12}h^3}{12} \varphi_{x,xy} + \frac{C_{22}h^3}{12} \varphi_{y,yy} + cc' \phi_y + \frac{C_{66}h^3}{12} \varphi_{x,xy} + \\ & \frac{C_{66}h^3}{12} \varphi_{y,xx} - C_{44}hw_{,y} - C_{44}h\varphi_{,y} - dd\phi_y + \\ & \frac{\nu h^2 \tau_s}{6(1-\nu)} \left(\frac{\partial^3 w}{\partial y^3} + \frac{\partial^3 w}{\partial y \partial x^2} \right) + \\ & (1-(e_0 a)^2 \nabla^2) E_s (bh^2/2 + h^3/6) \frac{\partial^2 \varphi_y}{\partial y^2} - \\ & 2\tau_s (1-(e_0 a)^2 \nabla^2) (b+h) \frac{\partial w}{\partial y} + \end{aligned} \tag{32b}$$

$$\begin{aligned} & E_{s,cm} (3\pi d^3/8) \frac{\partial^2 \varphi_y}{\partial y^2} + (1-(e_0 a)^2 \nabla^2) f_y^I = \\ & (1-(e_0 a)^2 \nabla^2) \left(\frac{\rho h^3}{12} + (bh^2/2 + h^3/6) \rho_s \right) \frac{\partial^2 \varphi_y}{\partial t^2} + \\ & \frac{\nu \rho_s h^2}{6(1-\nu)} \frac{\partial^3 w}{\partial t^2 \partial y} \\ & C_{44}hw_{,yy} + C_{44}h\varphi_{,yy} + dd\phi_{,yy} + C_{55}hw_{,xx} + C_{55}h\varphi_{,xx} + \\ & cc\phi_{,xx} + 4\tau_s (1-(e_0 a)^2 \nabla^2) (b+h) \left(\frac{\partial^2 w}{\partial x^2} + \frac{\partial^2 w}{\partial y^2} \right) + \\ & \frac{\nu h^2 \tau_s}{6(1-\nu)} \nabla^4 w + k_w (1-(e_0 a)^2 \nabla^2) w - k_g (1-(e_0 a)^2 \nabla^2) \nabla^2 w \\ & (1-(e_0 a)^2 \nabla^2) f_z^I - 4\tau_{s,cm} (1-(e_0 a)^2 \nabla^2) d \left(\frac{\partial^2 w}{\partial x^2} + \frac{\partial^2 w}{\partial y^2} \right) = \tag{32c} \\ & (1-(e_0 a)^2 \nabla^2) (\rho h + 2(b+h) \rho_s) \frac{\partial^2 w}{\partial t^2} + \\ & \frac{\nu \rho_s h^2}{6(1-\nu)} \left(\frac{\partial^4 w}{\partial t^2 \partial x^2} + \frac{\partial^4 w}{\partial t^2 \partial y^2} \right) \end{aligned}$$

$$\begin{aligned} & d_1 \varphi_{,x,x} + d_1 w_{,x,x} + d_2 \phi_{,x,x} + d_3 \varphi_{,y,y} + \\ & d_3 w_{,yy} + d_4 \phi_{,yy} + d_5 \varphi_{,x,x} + d_6 \varphi_{,y,y} - d_7 \phi = 0 \tag{32d} \end{aligned}$$

where

$$\begin{aligned} d_1 &= \int_{-h/2}^{h/2} e_{15} \cos\left(\frac{\pi z}{h}\right) dz, d_2 = \int_{-h/2}^{h/2} \xi_{11} \cos^2\left(\frac{\pi z}{h}\right) dz, \\ d_3 &= \int_{-h/2}^{h/2} e_{24} \cos\left(\frac{\pi z}{h}\right) dz, d_4 = \int_{-h/2}^{h/2} \xi_{22} \cos^2\left(\frac{\pi z}{h}\right) dz, \\ d_5 &= \int_{-h/2}^{h/2} \frac{\pi e_{31}}{h} z \sin\left(\frac{\pi z}{h}\right) dz, d_6 = \int_{-h/2}^{h/2} \frac{\pi e_{32}}{h} z \sin\left(\frac{\pi z}{h}\right) dz, \\ d_7 &= \int_{-h/2}^{h/2} \xi_{33} \left(\frac{\pi}{h}\right)^2 \sin^2\left(\frac{\pi z}{h}\right) dz \end{aligned} \tag{33}$$

Assuming that the boundary conditions are simply supported on all edges of the nanocomposite plate, Navier's type solution can be used to solve the motion equations as follows:

$$\begin{aligned} w(x, y) &= \sum_{i=1}^m \sum_{j=1}^n w_{mn} e^{i\omega t} \sin(m\pi x/a) \sin(n\pi y/b) \\ \varphi_x(x, y) &= \sum_{i=1}^m \sum_{j=1}^n \varphi_{xmn} e^{i\omega t} \cos(m\pi x/a) \sin(n\pi y/b) \\ \varphi_y(x, y) &= \sum_{i=1}^m \sum_{j=1}^n \phi_{ymn} e^{i\omega t} \sin(m\pi x/a) \cos(n\pi y/b) \\ \phi(x, y) &= \sum_{i=1}^m \sum_{j=1}^n \phi_{mn} e^{i\omega t} \sin(m\pi x/a) \sin(n\pi y/b) \end{aligned} \tag{34}$$

where m and n are the half axial and transverse wave numbers, respectively.

Substituting Eq. (34) into Eq. (32), the matrix form for the motion equations of nanocomposite plate can be expressed as follows:

for FSĐT:

$$\left(K - \omega^2 M \right) \begin{Bmatrix} w \\ \varphi_x \\ \varphi_y \\ \phi \end{Bmatrix} = 0 \tag{35}$$

where

$$K = \begin{bmatrix} K_{11} & K_{12} & K_{13} & K_{14} \\ K_{21} & K_{22} & K_{23} & K_{24} \\ K_{31} & K_{32} & K_{33} & K_{34} \\ K_{41} & K_{42} & K_{43} & K_{44} \end{bmatrix}, \quad (36a)$$

$$M = \begin{bmatrix} M_1 & 0 & 0 & 0 \\ M_2 & M_3 & 0 & 0 \\ M_4 & 0 & M_5 & 0 \\ 0 & 0 & 0 & 0 \end{bmatrix}$$

$$\lambda_1 = \frac{m\pi}{a}$$

$$\lambda_2 = \frac{n\pi}{b}$$

$$K_{11} = -C_{44}h\lambda_2^2 - \lambda_1^2 C_{55}h + k_w \left(1 + (e_0a)^2 (\lambda_1^2 + \lambda_2^2)\right) - 4\tau_s \left(1 + (e_0a)^2 (\lambda_1^2 + \lambda_2^2)\right) (b+h) (\lambda_2^2 + \lambda_1^2)$$

$$k_g \left(1 + (e_0a)^2 (\lambda_1^2 + \lambda_2^2)\right) (\lambda_1^2 + \lambda_2^2) + \frac{\nu h^2 \tau_s}{6(1-\nu)} (\lambda_2^2 + \lambda_1^2)^2 + 4\tau_{s_{cm}} \left(1 + (e_0a)^2 (\lambda_1^2 + \lambda_2^2)\right) (d_i + d_o) (\lambda_1^2 + \lambda_2^2) - \left(1 + (e_0a)^2 (\lambda_1^2 + \lambda_2^2)\right) (\eta h H_y^2 \lambda_2^2 + \eta h H_x^2 \lambda_1^2)$$

$$K_{12} = -\left(1 + (e_0a)^2 (\lambda_1^2 + \lambda_2^2)\right) \eta h H_y^2 \lambda_1 - C_{55}h\lambda_1$$

$$K_{13} = -C_{44}h\lambda_2 - \left(1 + (e_0a)^2 (\lambda_1^2 + \lambda_2^2)\right) \eta h H_x^2 \lambda_2$$

$$K_{14} = -dd\lambda_2^2 - cc\lambda_1^2$$

$$K_{21} = -C_{55}h\lambda_1 - \frac{\nu h^2 \tau_s}{6(1-\nu)} (\lambda_1^3 + \lambda_1\lambda_2^2) - 2\tau_s \left(1 + (e_0a)^2 (\lambda_1^2 + \lambda_2^2)\right) (b+h)\lambda_1$$

$$K_{22} = -\frac{C_{11}h^3}{12} \lambda_1^2 - \frac{C_{66}h^3}{12} \lambda_2^2 - C_{55}h - E_{s_{cm}} (3\pi (d_i^3 + d_o^3)/8) \lambda_1^2 - \left(1 + (e_0a)^2 (\lambda_1^2 + \lambda_2^2)\right) \frac{\eta h^3}{12} H_z^2 \lambda_1^2 - \left(1 + (e_0a)^2 (\lambda_1^2 + \lambda_2^2)\right) (\lambda_1^2 + \lambda_2^2) \frac{\eta h^3}{12} H_y^2 - E_s \left(1 + (e_0a)^2 (\lambda_1^2 + \lambda_2^2)\right) (bh^2/2 + h^3/6)$$

$$K_{23} = \left(-\frac{C_{12}h^3}{12} - \frac{C_{66}h^3}{12} + \left(1 + (e_0a)^2 (\lambda_1^2 + \lambda_2^2)\right) \left(\frac{\eta h^3}{12} H_z^2\right)\right) \lambda_1\lambda_2$$

$$K_{24} = (bb - cc)\lambda_1$$

$$K_{31} = -C_{44}h\lambda_2 - \frac{\nu h^2 \tau_s}{6(1-\nu)} (\lambda_2^3 + \lambda_1^2\lambda_2) - 2\tau_s \left(1 + (e_0a)^2 (\lambda_1^2 + \lambda_2^2)\right) (b+h)\lambda_2$$

$$K_{32} = \left(-\frac{C_{12}h^3}{12} - \frac{C_{66}h^3}{12} - \left(1 + (e_0a)^2 (\lambda_1^2 + \lambda_2^2)\right) \frac{\eta h^3}{12} H_z^2\right) \lambda_2\lambda_1$$

$$K_{33} = -\frac{C_{22}h^3}{12} \lambda_2^2 - \frac{C_{66}h^3}{12} \lambda_1^2 - \left(1 + (e_0a)^2 (\lambda_1^2 + \lambda_2^2)\right) \frac{\eta h^3}{12} H_z^2 \lambda_2^2 - C_{44}h - \left(1 + (e_0a)^2 (\lambda_1^2 + \lambda_2^2)\right) E_s (bh^2/2 + h^3/6) \lambda_2^2 - E_{s_{cm}} (3\pi (d_i^3 + d_o^3)/8) \lambda_2^2 - \left(1 + (e_0a)^2 (\lambda_1^2 + \lambda_2^2)\right) (\lambda_1^2 + \lambda_2^2) \frac{\eta h^3}{12} H_x^2$$

$$K_{34} = cc'\lambda_2 - dd\lambda_2$$

$$K_{41} = -d_1\lambda_1^2 - d_3\lambda_2^2$$

$$K_{42} = -(d_1 + d_5)\lambda_1$$

$$K_{43} = -(d_3 + d_6)\lambda_2$$

$$K_{44} = -d_2\lambda_1^2 - d_4\lambda_2^2 - d_7$$

$$M_1 = \left(1 + (e_0a)^2 (\lambda_1^2 + \lambda_2^2)\right) (\rho h + 2(b+h)\rho_s) - \frac{\nu\rho_s h^2}{6(1-\nu)} (\lambda_1^2 + \lambda_2^2)$$

$$M_2 = \frac{\nu\rho_s h^2}{6(1-\nu)} \lambda_1$$

$$M_3 = \left(1 + (e_0a)^2 (\lambda_1^2 + \lambda_2^2)\right) \left(\frac{\rho h^3}{12} + (bh^2/2 + h^3/6)\rho_s\right)$$

$$M_4 = \frac{\nu\rho_s h^2}{6(1-\nu)} \lambda_2$$

(36b)

For CPT:

$$(K - \omega^2 M) \begin{Bmatrix} w \\ \phi \end{Bmatrix} = 0 \tag{37}$$

where

$$K = \begin{bmatrix} K_{11} & K_{14} \\ K_{41} & K_{44} \end{bmatrix}, \quad M = \begin{bmatrix} M_{11} & 0 \\ 0 & 0 \end{bmatrix}$$

$$M_{11} = (1 + (e_0 a)^2 (\lambda_1^2 + \lambda_2^2)) (\rho h + 2(b+h)\rho_s) - \frac{\nu \rho_s h^2}{6(1-\nu)} (\lambda_1^2 + \lambda_2^2) - (1 + (e_0 a)^2 (\lambda_1^2 + \lambda_2^2)) \left(\frac{\rho h^3}{12} + (bh^2/2 + h^3/6)\rho_s \right) (\lambda_1^2 + \lambda_2^2) \tag{38}$$

To obtain the natural frequency for Eq. (39a), the determinant of coefficient matrix should be equal to zero:

$$|K - M \omega^2| = 0 \tag{39}$$

4. Results and discussion

Nanocomposite square plate made of polyvinylidene fluoride (PVDF) reinforced by SWCNTs is considered in this research. Due to piezoelectric property of PVDF and magnetic property of SWCNTs, these composite structures easily undergo the combined loadings. For validation of the research with other literatures, two steps are used as: firstly, using the properties of nano-plate which listed in Table 1, the natural frequencies of the square nonoplate with considering surface stress effect are compared with the obtained results by Ansari and Sahmani [7]. It is observed that there is a good agreement between them (Table 2).

Table 1. Surface and material properties of the square nano-plate

Material properties	
Young modulus	177.3GPa
Poisson's ratio	0.27
Density	7000 Kg / m ³
Residual surface stress constant	1.7 N / m
Lame surface stress constant	-3 N / m
Surface density	7e-6 Kg / m ²

Table 2. The non-dimensional fundamental frequencies of the square nano-plate (h=1nm)

b/h	ω_{11}		ω_{22}		ω_{33}	
	[7]	Present	[7]	Present	[7]	Present
10	1.003	1.003	1.023	1.023	1.056	1.0562
20	0.998	0.998	1.003	1.003	1.011	1.0106
30	0.997	0.997	0.999	0.999	1.003	1.003
40	0.997	0.997	0.998	0.998	1.000	1.000
50	0.997	0.997	0.997	0.997	0.999	0.999

In the second step, the non-dimensional fundamental natural frequencies of nanocomposite plate reinforced by SWCNT for various width to thickness ratio (b/h) and SWCNT volume fractions are listed in Tables 3 and 4, respectively. It can be shown the results are very closer to the obtained results by Zhu et al. [36]. Material properties, surface properties and geometry dimensions of piezoelectric nano-plate reinforced by SWCNT which are used in this research are listed in Table 5.

Table 3. The non-dimensional natural frequencies of composite plate reinforced by CNT

b/h	ω_{11}		ω_{22}		ω_{33}	
	[7]	Present	[7]	Present	[7]	Present
10	1.003	1.003	1.023	1.023	1.056	1.0562
20	0.998	0.998	1.003	1.003	1.011	1.0106
30	0.997	0.997	0.999	0.999	1.003	1.003
40	0.997	0.997	0.998	0.998	1.000	1.000
50	0.997	0.997	0.997	0.997	0.999	0.999

Table 4. The non-dimensional natural frequencies of composite plate reinforced by CNT

V_{CNT}	b/h	Present	[36]
0.11	10	13.5099	13.532
	20	17.3042	17.355
0.14	10	14.9106	14.306
	20	18.8946	18.921
0.17	10	16.7840	16.815
		43.0968	40.630
	20	21.3888	21.456

Table 5. Material properties, surface properties and geometry dimensions of square nano-plate reinforced by CNT

Parameters	PVDF	CNT
Elastic module	2.5GP	-
Poisson's ratio	0.3	0.175
Volume fraction	-	0.14
Residual surface stress constant	1.7 N/m	0.9108 N/m
Lame surface stress constant	4 N/m	5.1882 N/m
Orientation angle	-	0
Nonlocal parameter	0.5nm	0.5nm
Longitudinal elastic module	-	5.6466 TPa
Transverse elastic module	-	7.08 TPa
Shear module	-	1.9445 TPa
Length	20nm	20nm
Width	20nm	-
Thickness	2nm	-
Outer diameter	-	1.4940nm
Inner diameter	-	1.36nm

The effects of various parameters on the fundamental frequencies of piezoelectric square nano-plate reinforced by SWCNT are studied. E-M-T and E-M-R approaches are used to define material properties of piezoelectric nanocomposite plate.

Fig. 1 shows the non-dimensional frequency ratio ($\omega_{nonlocal} / \omega_{local}$) of piezoelectric nanocomposite plate versus SWCNT orientation angle for CPT and FSDT. As it can be seen that $\omega_{nonlocal} / \omega_{local}$ decreases with an

increase in SWCNT orientation angle up $\pi/4$ for CPT and vice versa for FSDT. Also $\omega_{nonlocal} / \omega_{local}$ decreases with increasing of the nonlocal parameter ($e_0 a$) for both plate theories. This fact is due to increasing atomic distance. The results of E-M-R approach are closer to E-M-T approach for FSDT with respect to CPT.

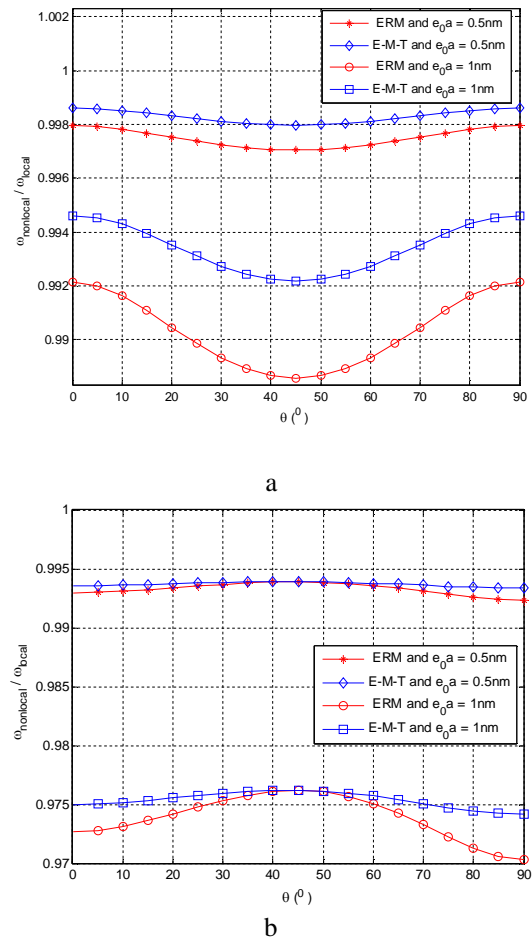


Fig. 1. $\omega_{nonlocal} / \omega_{local}$ of piezoelectric nanocomposite plate against CNT orientation angle for various nonlocal parameter values a- CPT b- FSDT

Fig. 2 depicts the effect of elastic foundation parameters on $\omega_{nonlocal} / \omega_{local}$ for FSDT and CPT. As it can be seen for both theories $\omega_{nonlocal} / \omega_{local}$ increases with the presence of

elastic foundation. Also it is clear that the results of $\omega_{nonlocal} / \omega_{local}$ for both E-M-R and E-M-T approaches are very closer together.

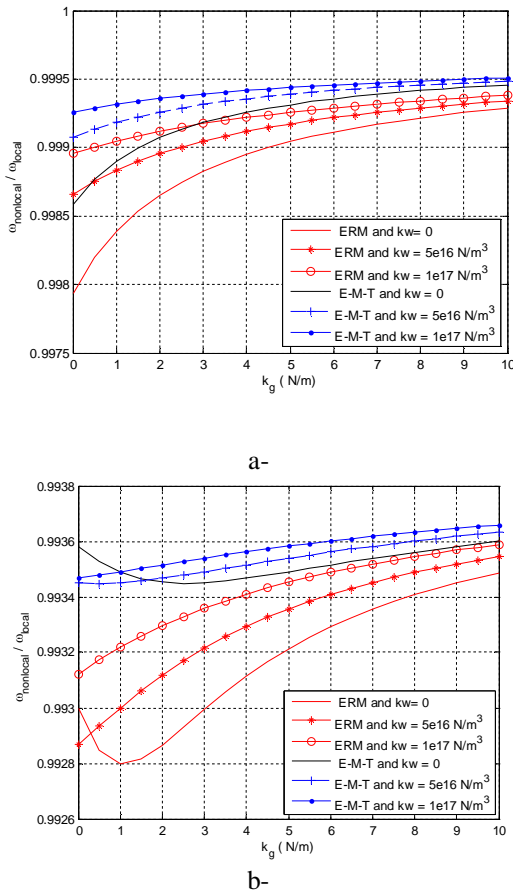


Fig. 2. $\omega_{nonlocal} / \omega_{local}$ of piezoelectric nanocomposite plate versus the shear constant (k_g) for various Winkler spring constant a- CPT b- FSDT

Fig. 3 illustrates the effects of applied magnetic field and voltage on $\omega_{nonlocal} / \omega_{local}$ for CPT and FSDT. It is concluded that $\omega_{nonlocal} / \omega_{local}$ increases with an increase in the applied magnetic field and voltage. As magnetic field in z direction and voltage are applied on piezoelectric nanocomposite plate, compressive loads are produced, then $\omega_{nonlocal} / \omega_{local}$ increases. Also

these effects on $\omega_{nonlocal} / \omega_{local}$ are higher for FSDT with respect to CPT. Also it is concluded that effect of applied magnetic field and voltage on $\omega_{nonlocal} / \omega_{local}$ for CPT are negligible.

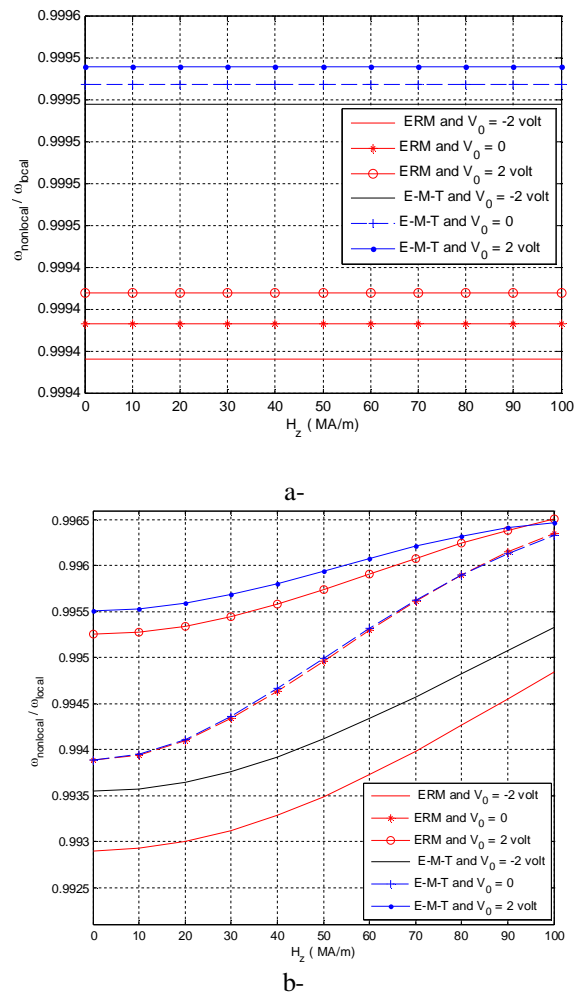
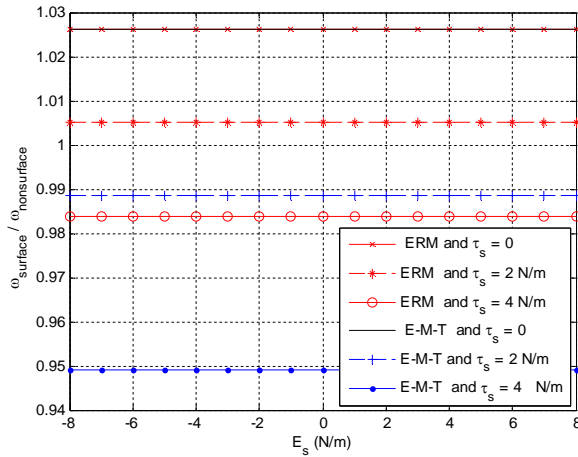


Fig. 3. $\omega_{nonlocal} / \omega_{local}$ of piezoelectric nanocomposite plate with respect to magnetic field intensity for various applied voltages a- CPT b- FSDT

Effects of nano-plate residual surface stress (τ_s) and surface Lamé constants (E_s) on surface fundamental frequency to non-surface fundamental frequency ($\omega_{surface} / \omega_{non-surface}$) are displayed in Figs. 4. It can be observed that

$\omega_{surface} / \omega_{nonsurface}$ increases with an increase in τ_s for both plate theories but effect of E_s on $\omega_{surface} / \omega_{nonsurface}$ isn't considerable.



a-

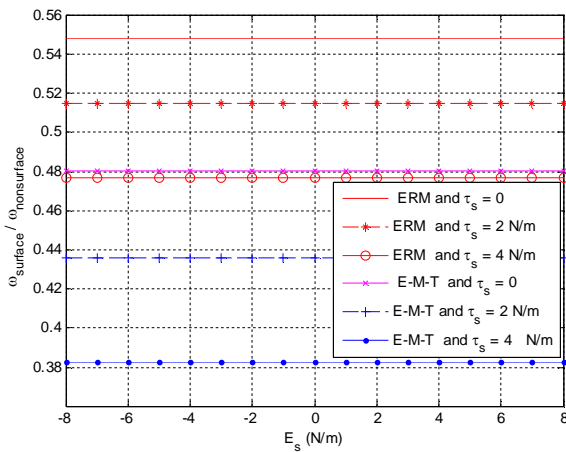


Fig. 4. Effects of residual surface stress constant and surface Lamé constant on $\omega_{surface} / \omega_{nonsurface}$ of piezoelectric nanocomposite plate a- CPT b- FSDT

Effects of residual surface stress constant and surface density (ρ_s) on $\omega_{surface} / \omega_{nonsurface}$ of piezoelectric nanocomposite plate for CPT are shown in Fig. 5. It is clear that $\omega_{surface} / \omega_{nonsurface}$ increases with increasing of ρ_s .

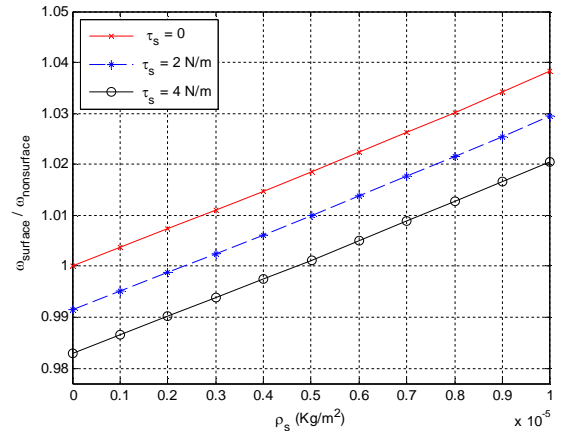


Fig. 5. Effects of residual surface stress constant and surface density on $\omega_{surface} / \omega_{nonsurface}$ of piezoelectric nanocomposite plate for CPT

Fig. 6 illustrates the influences of inclusion volume to total volume ratio (ξ) and SWCNT volume fraction in the inclusion (ζ) ratios on $\omega_{nonlocal} / \omega_{local}$ of piezoelectric composite plate for CPT and FSDT. It is concluded that $\omega_{nonlocal} / \omega_{local}$ decreases with increasing of ζ and vice versa for ξ . As ζ increases, the SWCNT accumulation in PVDF increases hence $\omega_{nonlocal} / \omega_{local}$ decreases.

In Fig. 7, effects of the nonlocal parameter and aspect ratio (a/b) on $\omega_{nonlocal} / \omega_{local}$ of piezoelectric nanocomposite plate for CPT and FSDT using the E-M-R are demonstrated. As it can be seen that difference of $\omega_{nonlocal} / \omega_{local}$ in higher nonlocal parameter for FSDT is higher than that of for CPT.

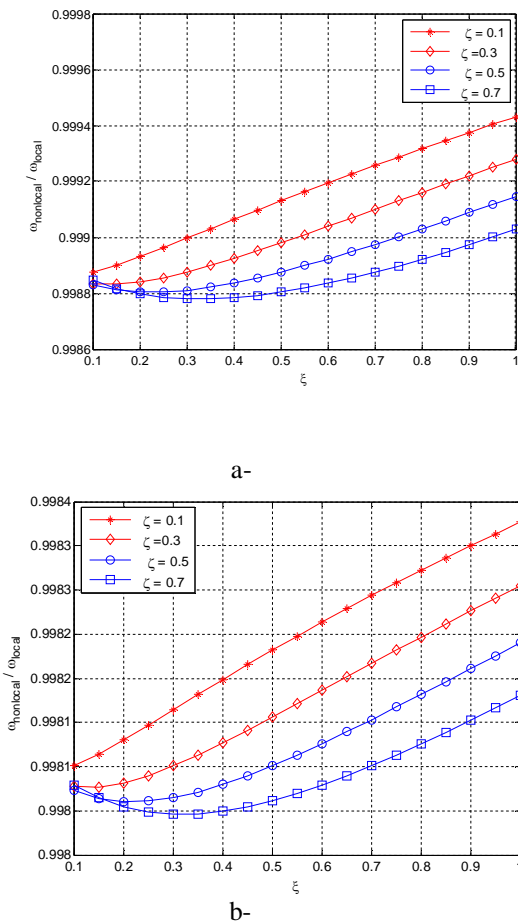


Fig. 6. Agglomeration effects on $\omega_{nonlocal} / \omega_{local}$ of piezoelectric nanocomposite plate a- CPT b- FSDT

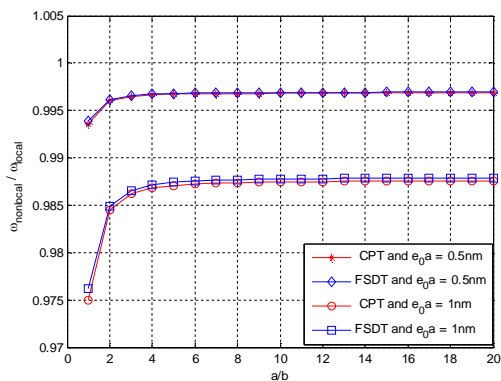


Fig. 7. Effects of the nonlocal parameter and aspect ratio on $\omega_{nonlocal} / \omega_{local}$ of piezoelectric nanocomposite plate for CPT and FSDT using the extended mixture rule

5. Conclusions

In this article, the free vibration analysis of piezoelectric nanocomposite plate reinforced by SWCNT based on CPT and FSDT is studied. The extended mixture rule and Eshelby-Mori-Tanaka approaches are employed to obtain elastic properties of the nanocomposite. The motion equations are derived by energy method and Hamilton principle. Navier 's method is used to obtain the natural frequency of piezoelectric nanocomposite plate. Influences of the nonlocal parameter, aspect ratio, SWCNT volume fraction, SWCNT orientation angle, surface stress parameters, elastic foundation parameters, magnetic fields and external applied voltage, SWCNT agglomeration effect and surface stress effect on the non-dimensional frequency ratio of piezoelectric nanocomposite plate are investigated. The results of this research can be stated as follows:

- 1- The nonlocal fundamental frequency to local fundamental frequency ratio ($\omega_{nonlocal} / \omega_{local}$) of piezoelectric nanocomposite plate increases with an increase in volume fraction of SWCNT, aspect ratio of b/h , aspect ratio of a/b , elastic foundation parameters, applied voltage, magnetic field and inclusion volume to total volume ratio (ξ).
- 2- $\omega_{nonlocal} / \omega_{local}$ of piezoelectric nanocomposite plate decreases with increasing of SWCNT orientation angle for CPT, SWCNT volume fraction in the inclusion (ζ) and the nonlocal parameter.
- 3- Increasing of $\omega_{nonlocal} / \omega_{local}$ of piezoelectric nanocomposite plate with the positive applied voltage is more than that of with negative applied voltage.

- 4- The surface frequency to non-surface frequency ratio ($\omega_{surface} / \omega_{nonsurface}$) of piezoelectric nanocomposite plate increases with increasing of surface density.
- 5- $\omega_{surface} / \omega_{nonsurface}$ of piezoelectric nanocomposite plate decreases with increasing of residual surface stress constant.

Acknowledgments

The authors would like to thank the referees for their valuable comments and the Iranian Nanotechnology Development Committee for their financial support. They are also grateful to the University of Kashan for supporting this work by Grant No. 363452/6.

References

- [1] R.H. Baughman, A. A. Zakhidov, W. A De Heer, *Sci.* 297 (2002), p. 787.
- [2] T. Murmu, M. A. McCarthy, S. Adhikari, *Compos. Struct.* 96 (2013), 57–63.
- [3] R. Aghababaei, J. N. Reddy, *J. Sound Vib.* 326 (2009), 277–289.
- [4] R. Ansari, R. Rajabiehfard, B. Arash, *Comput. Mater. Scie.* 49 (2010), 831–838.
- [5] A. Ghorbanpour Arani, S. Amir, A. R. Shajari, M.R. Mozdianfard, Z. Khoddami Maraghi, M. Mohammadimehr, *Proc Institue Mech. Eng .Part C* 224 (2011), 745,756.
- [6] K. F.Wang, B. L.Wang, *Physica E* 44 (2011), 448–453.
- [7] R. Ansari, S. ahmani, *Int. J. Eng. Sci.* 49 (2011), 1204–1215.
- [8] K. F.Wang, B. L. Wang, *Int. J. Non Linear Mech.* 55 (2013), 19–24.
- [9] E. Jomehzadeh, A. R. Saidi, *Compos. Struct.* 93 (2011), 1015–1020.
- [10] T. Aksencer, M. Aydogdu, *Physica E* 43 (2011), 954–959.
- [11] M. Mohammadimehr, A. M. Rahmati, *Turkish J. Eng. Env. Sci.* 37 (2013), 1–15.
- [12] T. Aksencer, M. Aydogdu, *Physica E* 44 (2012), 1752–1759.
- [13] B. Akgz, Q. Civalek, *Mater. Des.* 42 (2012), 164–171.
- [14] Z. B. Shen, H. L. Tang, D. K. Li, G. J. Tang, *Comput. Mater. Sci.* 6 (2012), 200–205.
- [15] A. Shakouri, T. Y. Ng, R. M. Lin, *Physica E* 50 (2013), 22–28.
- [16] Sh. Hashemi, M. Zare, R. Nazemnezhad, *Compos. Struct.* 100 (2013), 290–299.
- [17] K.F. Wang, B.L. Wang, *Finite Elem. Anal. Des.* 74 (2013), 22–29.
- [18] A.H. Rahmati, M.Mohammadimehr, *Physica B* 440 (2014), 88–98.
- [19] P. Malekzadeh, M. Shojae, *Compos. Struct.* 95 (2013), 443–452.
- [20] T. Murmu, S. C.Pradhan, *Physica E* 41 (2009), 1628–1633.
- [21] Ch. Liu, L. L. Ke, Y. Sh.Wang, J. Yang, S. Kitipornchai, *Compos. Struct.* 106 (2013), 167–174.
- [22] C. Zhang, W. Chen, Ch. Zhang, *Eur. J. Mech. A. Solids* 41 (2013), 50-57.
- [23] S.C. Pradhan, A. Kumar, *Compos. Struct.* 93 (2011), 774–779.
- [24] P. Malekzadeh, A. R. Setoodeh, *Compos. Struct.* 93 (2011), 1631–1639.
- [25] A. Ghorbanpour Arani, Sh. Maghamikia, M. Mohammadimehr, A. Arefmanesh, *J Mech Sci Technol* 25 .3 (2011), 809-820.
- [26] S. Poursmaeeli, S. A.Fazelzadeh, E. Ghavanloo, *Composites: Part B* 43(2012), 3384–3390.

- [27] A. R. Shahidi, A. Anjomshoa, S. H. Shahidi, M. Kamrani, *Appl. Math. Modell.* 37 (2013), 7047–7061.
- [28] G. Formica, W. Lacarbonara, R. Alessi, *J. Sound Vib.* 329 (2010), 1875–1889.
- [29] S. U. Khan, C. Y. Li, N. A. Siddiqui, J. K. Kim, *Compos. Sci. Technol.* 71 (2013), 1486–1494.
- [30] Z. X. Lei, K. M. Liew, J. L. Yu, *Compos. Struct.* 106 (2013), 128–138.
- [31] H. S. Shen, *Compos. Struct.* 91 (2009), 9-19.
- [32] D. L. Shi, X.Q. Feng, Y. Y. huang, K. C. Hwang, H. Gao, *J. Eng. Mat. Technol.* 126 (2004), 250-257.
- [33] S. Jafari Mehrabadi, B. Sobhani Aragh, V. Khoshkhahesh, A. Taherpour, *Composit.: Part B* 43 (2012), 2031–2040.
- [34] L. Wang, *Physica E* 44 (2012): 808–812.
- [35] J. Kraus, *Electromagnetics.* USA: McGrawHill Inc1984.
- [36] P. Zhu, Z. X. Lei, K. M. Liew, *Compos. Struct.* 94 (2012), 1450–1460.